Int. J. Electrochem. Sci., 16 **(2021)** Article ID: 210546, doi: 10.20964/2021.05.26

International Journal of
ELECTROCHEMICAL
SCIENCE
www.electrochemsci.org

Enhanced Photocatalytic Degradation of Azo Dye by Metal co-doped ZnO Nanorods under Ultraviolet Light Irradiation

Min Wang[1], *Shaochun Yuan*[1,2,*], *Bo Lv*[2,*], *Dongcai He*[3]

[1] School of River and Ocean Engineering, Chongqing Jiaotong University, Chongqing, 400074, PR China
[2] Engineering Research Center for Sponge City Construction of Chongqing, Chongqing, 400020, PR China
[3] Shenzhen Municipal Design & Research Institute Co., Ltd, Shenzhen, 518029, PR China
[*]E-mail: yuansc@cqjtu.edu.cn (Shaochun Yuan) and haimiancq@163.com (Bo Lv)

Received: 5 Janary 2021 / *Accepted:* 28 February 2021 / *Published:* 31 March 2021

Copper (Cu)–Nickel (Ni) co-doped ZnO nanorods (NRs) were synthesized via simple hydrothermal technique on fluorine-doped tin oxide (FTO) glass substrate. The structural, morphological, electrochemical and photocatalyst properties of prepared specimens were considered by SEM, XRD, electrochemical and photodegradation analyses. The SEM results showed that hexagonal wurtzite structure and high density of co-doped ZnO NRs were successfully synthesized on FTO substrate. The XRD findings indicate that crystallite size of the doped or co-doped specimens reduces due to Cu and Ni incorporation, showing that the Cu or Ni doping reserved crystal growth of ZnO nanostructure. The EIS results reveal that smaller resistance of Cu–Ni co-doped ZnO NRs than the other samples was found, which confirm the enhancement of ZnO conductivity by doping metal ions in ZnO structures because of the synergistic effect between metal and ZnO NRs. Optical absorption spectrum indicates that doping procedure increases the value of absorption in the UV-region which can be associated with the narrower band-gap of metal oxides toward the band-gap of pure ZnO. Photocatalytic behavior of Cu–Ni co-doped ZnO NRs revealed that the presence of both Cu and Ni dopants into ZnO causes the production of photoexcited electron-hole pairs in ZnO nanostructures under UV-light, which lead to significantly increased the free-carrier concentration, activated radicals and facilitated the generation of robust oxidizing hole, and finally accelerated azo dye removal and degradation. These findings show that Cu-Ni co-doped ZnO NRs with tuned optical properties can be promising candidates for applications in ceramics, optoelectronic devices and photocatalytic activity.

Keywords: Photocatalyst property; Metal co-doped ZnO nanorods; Hydrothermal technique; azo dyes; Electrochemical impedance spectroscopy

1. INTRODUCTION

In industrialized countries, pollutant associated with industrial wastewater, such as leather, textile, petrochemical, coatings, and paper industries, have caused environmental issues such as soil

and water pollution[1, 2]. Various techniques, including reverse osmosis, ultra filtration, silica gel, wood chips, and adsorption on various materials have been reported to eliminate toxins from industrial wastewater[3, 4].

Among the various developing methods dealing with the environmental and energy problems, the photocatalysis suggests several benefits such as reusable, facile and complete removal of dyes from wastewater without producing any damage to the environment [5-7]. Therefore, photocatalysis is studied as agreen chemical, efficient and promising technique.

Semiconductor materials are of interest to scientists because of their essential roles in optical, catalytic, electrical and magnetic applications [8, 9]. Though, the size-dependent properties of semiconductors offer a significant opportunity to produce new peculiar devices[10].

Zinc oxide (ZnO) is a semiconductor applied for many applications such as photocatalytic activity, piezoelectric transducers, transparent conducting films and gas sensor [11]. It can be synthesized with well-defined types of nanostructures such as nanobelts, nanotubes, nanonails, nanorods and nanowires[12, 13]. Furthermore, optical and structural properties of metal oxides are amended by doping transition metals.

The existence of two transition metal ions in ZnO is investigated as a favorable alternative method to attain stable magnetic and optical properties[14]. Many metal ions such as Co, Mn, Fe, Bi, Al and Ni have been doped in ZnO to improve its performance as a photocatalyst [15, 16]. Thus, researchers have made an effort to simultaneously doping two transition metal ions in ZnO. Co-dopant ions select depending on the individual magnetic contribution, coordination number, valence states and ionic radius [17, 18]. In this study, we considered the role of copper (Cu) and nickel (Ni) ions in ZnO nanorods (NRs). Photocatalytic properties of metal co-doped ZnO nanostructures have been studied by various research groups. But, development of Cu–Ni co-doped ZnO NRs, its enhanced photocatalytic behavior, and degradation of azo dye under UV irradiation are still controversial. Therefore, this work aims to prepare the Cu–Ni co-doped ZnO NRs using facile hydrothermal technique. The influence of Cu and Ni dopants on morphological, structural, photoluminescence and UV–visible properties of ZnO NRs were investigated. Furthermore, the photocatalytic test exhibited superior efficiency of Cu–Ni co-doped ZnO photocatalyst.

2. MATERIALS AND METHODS

In order to prepare metal co-doped ZnO nanorods, a typical hydrothermal route was utilized to grow Cu (copper)-Ni (nickel) co-doped ZnO nanorods on the fluorine-doped tin oxide (FTO) substrate. First, FTO substrate was cleaned in acetone for 10 min, 10 min in ethanol, and then 10 min in DI water. All steps were done in an ultrasonic-bath. After that, the glass substrates were dried through a N_2 gas flux. After that, ZnO seed-layers were produced by a sol−gel technique on FTO substrates. For seed-layer production, a solution with zinc acetate dehydrates (0.5 M) and monoethanolamide within a 1:1 molar ratio in ethanol solution was prepared. The mixture was transferred into an ultrasonic-bath at 50°C for 30 min and was maintained stirring at 50°C for an extra 30 min. Then, the precursor solutions were permitted to cool down to ambient temperature, and then, 250μL of solution was put on FTO

through spin-coating at 3000 rpm for 20 s. Finally, the films were annealed by a hot plate at 400°C for 10 min in air.

After the creation of the seed-layer, ZnO nanorods were synthesized on substrates by hydrothermal technique. The prepared substrates with a seed-layer were put upside down into a glass beaker containing aqueous solution of 0.1M zinc nitrate hexahydrate ($Zn(NO_3)_2.6H_2O$) and 0.1M hexamethylenetetramine (HMT) and heated at 80°C for 3 h, then cleaned with DI water and dried.For preparation of Cu-Nico-doped ZnO nanorods, nickel nitrate hexahydrate and copper nitrate trihydrate solution as precursor and doping sources were used. Then, nickel nitrate and/or copper nitrate solutions were mixed into 0.1M zinc nitrate hexahydrate solution (5:95) to synthesize doped and co-doped specimens according to ZnO nanorods growth as mentioned above.

The morphology of prepared samples was considered by scanning electron microscopy (SEM). The X-ray diffract-meter with Cu Kα radiation at wavelength of 1.5404Å operating at 30 kV and 20 mA was used to investigate the crystal structures of specimens. EIS tests were done in frequency range from 0.1 kHz to 1 MHz at 5 mV AC voltage using CHI 660D potentiostat (Chenhua Co. Shanghai, China) in a conventional three-electrode electrochemical cell which included prepared metal doped ZnO/FTO electrode, Pt wire and Ag/AgCl electrode as working, counter and reference electrodes, respectively. The electrolyte solution was in 0.1M KCl (99%) including 5mM complex $[Fe(CN)_6]^{3-/4-}$ (99.5%) solution. Photo-catalysis tests were performed by a photoreaction tool (15 Watt UV Bench Lamp) as a UV-light source. The concentration of azo dyes is 25 mg/L. The UV/Vis spectrophotometer (UV-2100, China) was used to measure the absorbance spectra of the MB solution.

3. RESULTS AND DISCUSSION

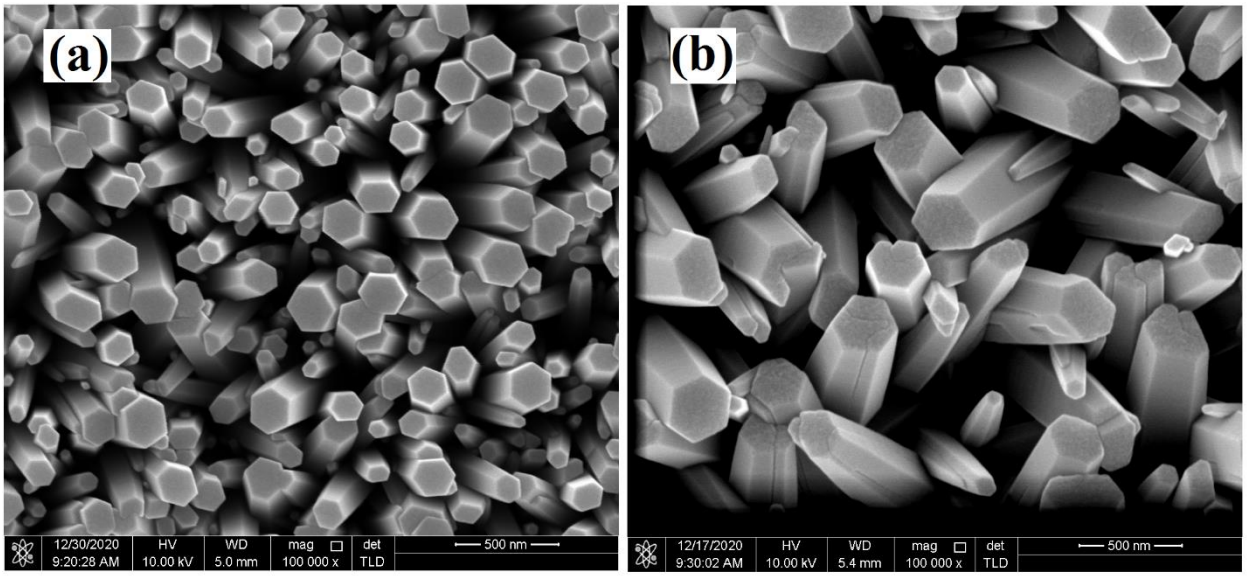

Figure 1. FESEM images of (a) ZnO (b) Cu–Ni co-doped ZnO nanorods prepared with hydrothermal method on FTO glass

FESEM images of the ZnO nanorods prepared through hydrothermal method are revealed in Figure 1. As shown, Cu–Ni co-doped ZnO nanorods are formed on FTO glass substrate in average length and diameter of 1.4µm and 150 nm, respectively which show the high uniform and density of the created ZnO nanostructures on FTO substrate. The samples indicate the common growth structure of crystal-like hexagonal shapes. Thus, high density and high aspect ratio of co-doped ZnO nanorods indicate high effective surface-area was shaped on FTO substrate.

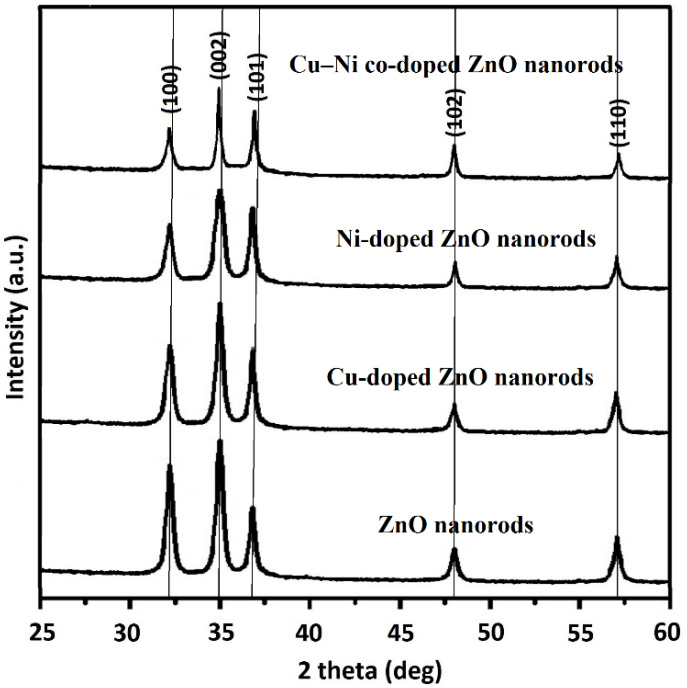

Figure 2. XRD patterns of various samples

Figure 2 indicates XRD patterns of pure ZnO nanorods, Cu–doped ZnO nanorods, Ni-doped ZnO nanorods and Cu–Ni co-doped ZnO nanorods. The obtained peaks of all specimens confirm the hexagonal wurtzite structure of ZnO nanorods as stated by JCPD Card No.36–1451[19]. The XRD patterns of doped and co-doped ZnO reveal that there are only zinc oxide peaks without any because ofCu or Ni or metal oxides (Cu_2O_3 or Ni_2O_3) phases. Furthermore, there isn't any peak shift to the higher or lower angle in doped ZnO nanorods, only a slight decrease in the intensity of diffraction peak is detected. The Debye-Scherrer equation was utilized to determine average crystallite size of the samples which estimated to be 30 nm for undoped ZnO and 24 nm, 27 nm and 22 nm for Cu–doped ZnO, Ni-doped ZnO and Cu–Ni co-doped ZnO nanorods, respectively. These results exhibit that crystallite size of the doped or co-doped specimens reduces due to Cu and Ni incorporation, showing that the Cu or Ni doping reserved crystal growth of ZnO nanostructure.

EIS assessments were done to consider samples in frequency range of 0.1Hz to 0.1 MHz at 5 mV applied voltage in 0.1M KCl (99%) including 5mM complex $[Fe(CN)_6]^{3-/4-}$ (99.5%) solution.

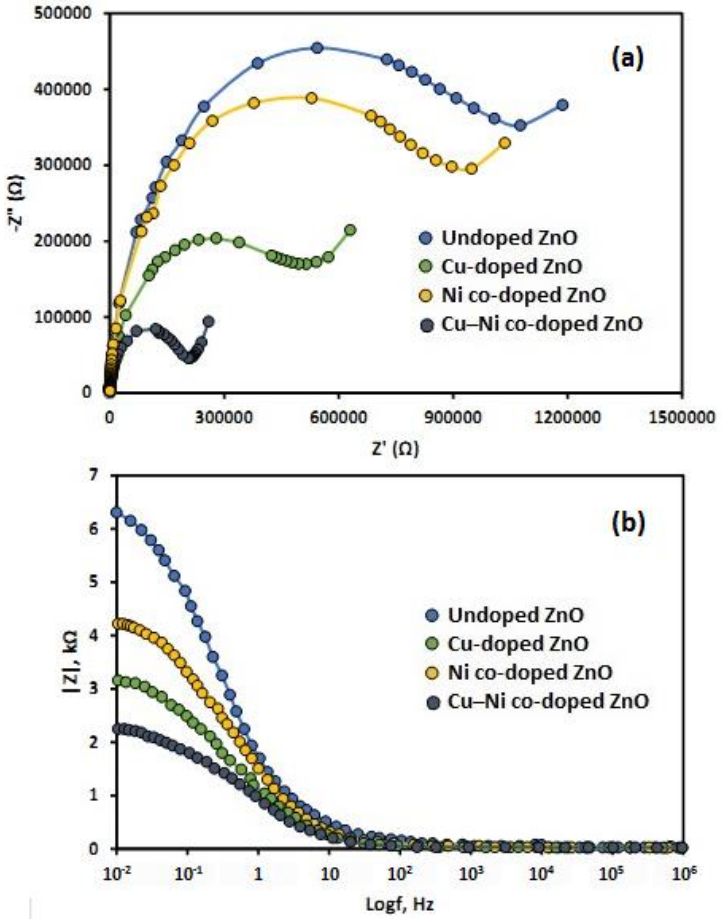

Figure 3. (a) The Nyquist diagrams and (b) Bode plots of undoped ZnO nanorods, Cu-doped ZnO nanorods, Ni-doped ZnO nanorods and Cu–Ni co-doped ZnO nanorods with frequency range of 0.1Hz to 0.1 MHz at 5 mV applied voltage in 0.1M KCl (99%) including 5mM complex $[Fe(CN)_6]^{3-/4-}$(99.5%) solution.

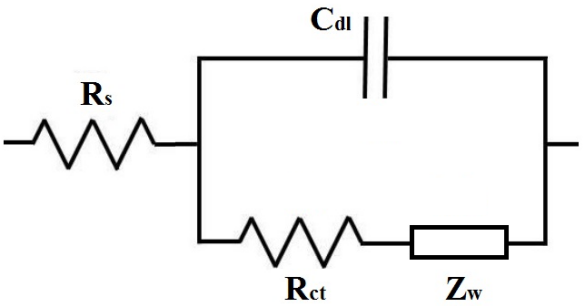

Figure 4. Equivalent circuit utilized for the impedance spectra

Figure 4 reveals the Nyquist diagram and Bode plot of undoped ZnO nanorods, Cu-doped ZnO nanorods, Ni-doped ZnO nanorods and Cu–Ni co-doped ZnO nanorods. The impedance results were received by the employed Randles equivalent circuit as shown in Figure 4 [20]. Rct and C_{dl} are the resistances of charge-transfer and the capacitances of double-layer, respectively. Rs is the resistance of solution.

Table 1. Electrochemical parameters obtained from the equivalent circuit (Fig. 4) for various specimens

Samples	R_s (Ω cm^2)	R_{ct} (MΩ cm^2)	C_{dl}(μF cm^{-2})
UndopedZnO	64.2	1.21	8.2
Cu-doped ZnO	53.8	0.57	12.3
Ni-doped ZnO	51.7	1.08	9.6
Cu-Ni co-doped ZnO	61.6	0.28	19.2

All samples show similar nature, having a semicircle loop at high frequency and straight line at low frequency regions. Charge-transfer resistance (R_{ct}) may be correlated to the semicircle and the straight line signifies diffusion or transport of electrolyte ions to the electrode surface [21]. As shown in table 1, the Cu–Ni co-doped ZnO nanorods were obviously exhibited lower R_{ct} value than the other samples, which related to enhancement of the conductivity of ZnO NRs by doping metal ions in ZnO nanostructures because of the synergistic effect between metal and ZnO nanorods [22]. Moreover, high electron-transfer rate may be associated with more interfaces between Cu, Ni and ZnO [23]. On the other hand, the increase of the electrical conductivity for the co-doped ZnO nanorods may be due to the redox-mediated formation with Cu and Ni [24].

The UV-vis spectroscopy was used to assess the optical properties of metal co-doped samples. Figure 5a indicates the recorded absorption spectrum of the metal co-doped ZnO nanorods in the wavelength range of 280-780 nm. As revealed, the maximum and comparatively low absorption phenomena are happen in the UV-region (280-350 nm) and visible-region for all specimens, respectively.

Furthermore, it is found that doping procedures increase the value of absorption in the UV-region which can be associated with the narrower band-gap (E_g) of metal oxides toward the band-gap of pure ZnO. The Tauc technique was used to calculate the band-gap values in Fig.4b with the following equation [25]:

$$\alpha h\nu = A(h\nu - E_g)^{1/2} \qquad (1)$$

Where αpresents the coefficient of optical absorption and h, ν and A are Planck's constant, frequency and energy independent constant, respectively. As observed in Fig. 5b, E_g of undoped ZnO, Cu-doped ZnO, Ni-doped ZnO and Cu–Ni co-doped ZnO nanorods were obtained 3.18, 3.27, 3.06, 3.14 and 2.98 eV, respectively. Thus, increasing the concentration of dopant causes a reduction in the band-gap of the specimens. Moreover, electrons and holes can be created in the semiconductor band structure under UV-vis light irradiation. The photo-generated charge-carrier may enhance the photocatalytic activities [11, 26, 27]. As a result, doping procedures with metals can prevent the recombination of holes and electrons, improving the catalytic activities and make robust light-harvesting abilities.

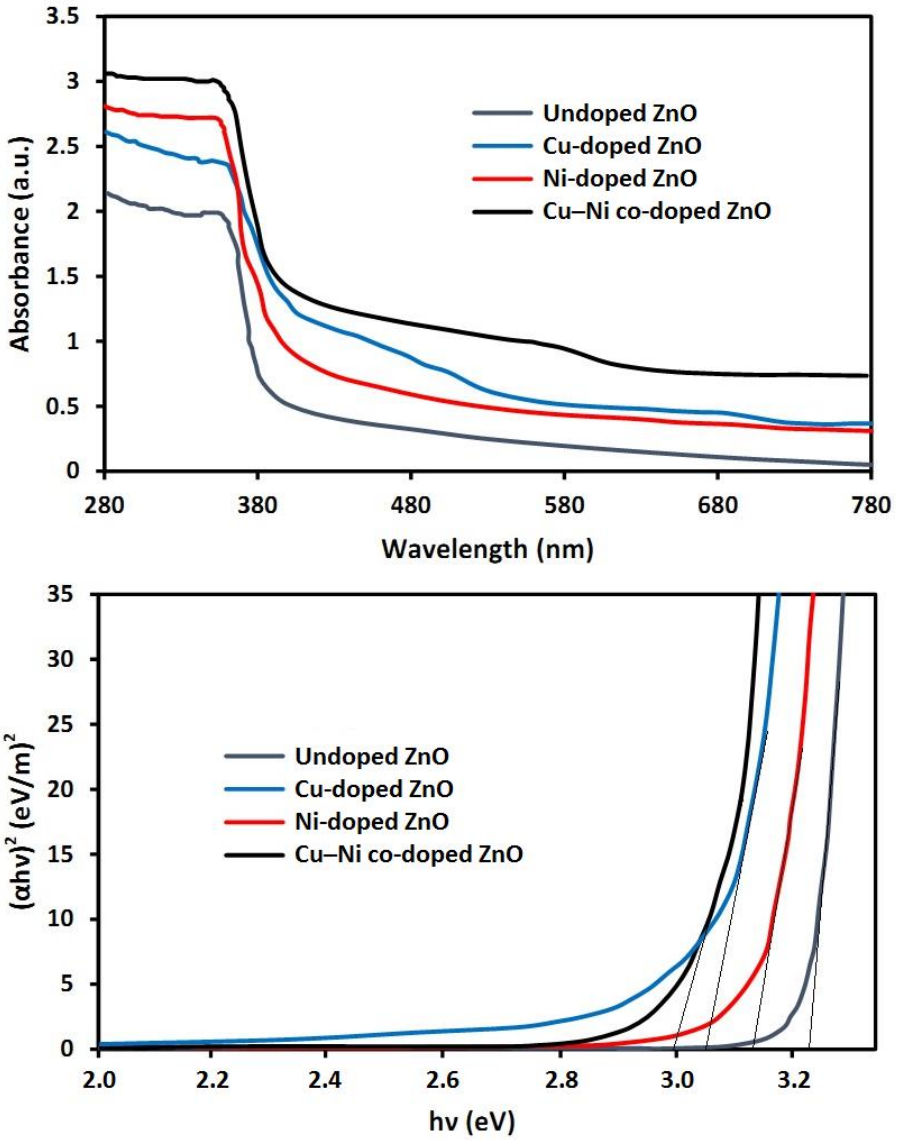

Figure 5. (a) Optical absorption spectrum and (b) Tauc plots of various samples at room temperature

In order to comparative study on the photocatalytic degradation of Cu–Ni co-doped ZnO nanorods in UV irradiation, the direct UV radiation (Blank), ZnO, Cu-doped ZnO and Ni-doped ZnO were used.

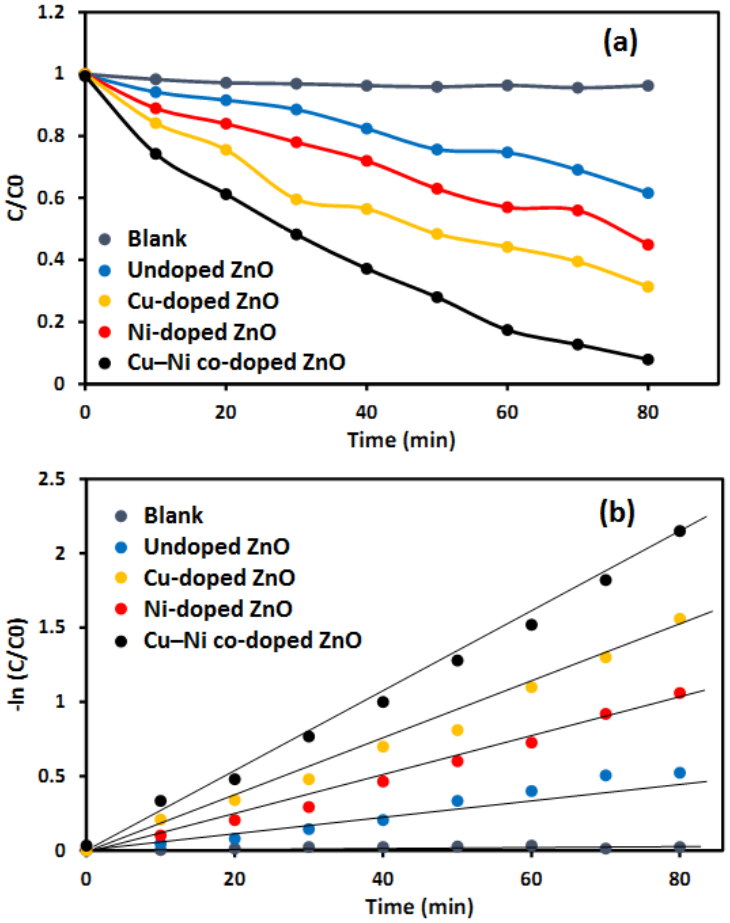

Figure 6. (a) Photodegradation and (b) Degradation rate of 10 mgl^{-1} azo dye on various electrodes under UV irradiation

As shown in Figure 6a, the azo dye concentration of the blank had no variation under UV light which indicated that azo dye is difficult to degrade by only UV radiation. After metal doping, azo dye degradation was noticeable, which confirmed that azo dyes were removed through catalyst under UV light. The degradation efficiency of Cu–Ni co-doped ZnO nanorods was considerably higher than degradation efficiency of the other samples. After 80 minutes of UV irradiation, the removal efficiency of azo dye reached 92%.As sown in Figure 6b, the $-\ln C_t/C_0$ regarding each photocatalyst was fundamentally linear related to reaction time (t), hence revealing that degradation of azo dye followed the Pseudo-1st-order reactions. The reaction rate coefficient (k) of blank, ZnO, Cu-doped ZnO, Ni-doped ZnO and Cu–Ni co-doped ZnO are 0.0002, 0.0071, 0.0185, 0.0131 and 0.0261 min^{-1}, respectively. Cu–Ni co-doped ZnO had the strongest UV photocatalytic activities. Compared with undoped ZnO, the performance of photocatalytic degradation was considerably improved by the metal doping. Dopant enhanced the UV-absorption of ZnO nanorods. The synthesized Cu–Ni co-doped ZnO had regular and uniform morphologies, and more adsorption active site was appeared on every crystal surface, which was favorable to the use of UV radiation and the adsorption of azo dye. The presence of both Cu and Ni dopants into ZnO nanorods causes the production of photoexcited electron-hole pairs in ZnO nanostructures under UV-light. It can cause the separation of holes and electrons and then slow

down their recombination [28]. Furthermore, Cu–Ni co-doped ZnO nanorods can better make more catalytic current than the other samples under UV light. Therefore, it significantly increased the free-carrier concentration, activated radicals and facilitated the generation of robust oxidizing hole, and finally accelerated azo dye removal and degradation [29].

Figure 7 shows the azo dye degradation efficiency on Cu–Ni co-doped ZnO NRs surface for different azo dye concentrations under UV irradiation. The degradation performance of approximately100% for 10, 20, 40 and 80 mgl^{-1} of azo dye occurs after 70, 90, 120 and 160 min under UV light, respectively. Table 2 indicates a comparison between the removal performance of this photocatalyst and other reported catalysts for azo dye degradation under UV-light. As observed, the prepared Cu–Ni co-doped ZnO nanorods exhibited comparable photocatalytic performance for removal of azo dye under UV irradiation. The co-doped ZnO nanorods can excite upon UV radiation and the photoexcited-carrier of valence and conduction bands and may react withO_2 and H_2O/OH^- molecules on the photocatalyst surface and active species induce such as O_2^- and $^{\bullet}OH$ radicals [30, 31].

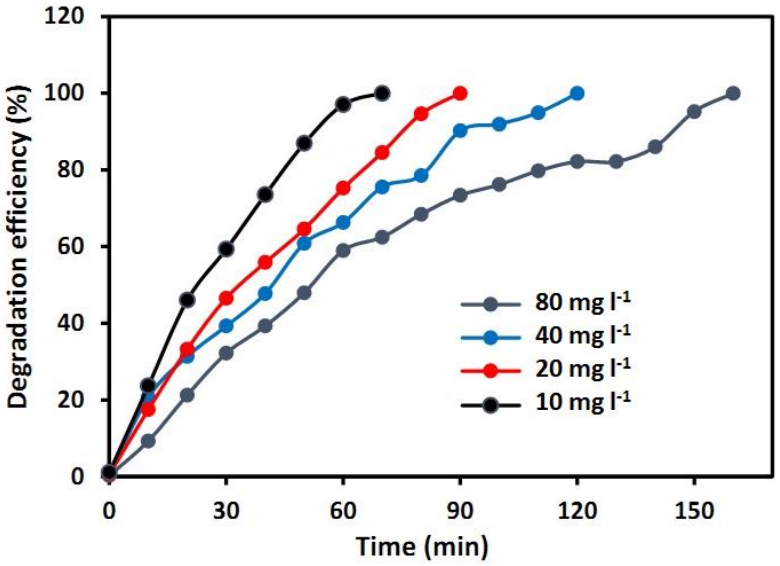

Figure 7. The azo dye degradation efficiency on Cu–Ni co-doped ZnO nanorods for different azo dye concentrations under UV radiation

Table 2. A comparison study between the removal performance of this photocatalyst and other reported catalysts for azo dye degradation under UV-light

Catalysts	azo dye content (mgl^{-1})	Degradation efficiency (%)	Radiation time (min)	Ref.
Ru-Modified ZnO	20	92	360	[32]
Mn-doped ZnO	10	84	390	[33]
Ag-doped ZnO	400	93	30	[34]
Ni-doped ZnO	50	93	120	[35]
Cu–Ni co-doped ZnONRs	10	100	70	This study

4. CONCLUSIONS

Cu–Ni co-doped ZnO NRs was synthesized via simple hydrothermal technique on FTO glass substrate. The structural, morphological, electrochemical and photocatalyst properties of prepared specimens were considered by SEM, XRD, electrochemical and photodegradation analyses. The SEM results showed that hexagonal wurtzite structure and high density of co-doped ZnO NRs were successfully synthesized on FTO substrate. The XRD findings indicate that crystallite size of the doped or co-doped specimens reduces due to Cu and Ni incorporation, showing that the Cu or Ni doping reserved crystal growth of ZnO nanostructure. The EIS results reveal that smaller resistance of Cu–Ni co-doped ZnO NRs than the other samples was found, which confirm the enhancement of ZnO conductivity by doping metal ions in ZnO structures because of the synergistic effect between metal and ZnO NRs. Optical absorption spectrum indicates that doping procedure increases the value of absorption in the UV-region which can be associated with the narrower band-gap of metal oxides toward the band-gap of pure ZnO. Photocatalytic behavior of Cu–Ni co-doped ZnO NRs revealed that the presence of both Cu and Ni dopants into ZnO causes the production of photoexcited electron-hole pairs in ZnO nanostructures under UV-light, which lead to significantly increased the free-carrier concentration, activated radicals and facilitated the generation of robust oxidizing hole, and finally accelerated azo dye removal and degradation.

ACKNOWLEDGEMENT
The authors are grateful for the financial support provided by the Natural Science Foundation of Chongqing (cstc2020jcyj-msxmX1000), Chongqing Construction Technology Plan Project (2020-5-7).

References

1. R. Kishor, D. Purchase, G.D. Saratale, R.G. Saratale, L.F.R. Ferreira, M. Bilal, R. Chandra and R.N. Bharagava, *Journal of Environmental Chemical Engineering*, 15 (2021) 105012.
2. H. Karimi-Maleh, Y. Orooji, A. Ayati, S. Qanbari, B. Tanhaei, F. Karimi, M. Alizadeh, J. Rouhi, L. Fu and M. Sillanpää, *Journal of Molecular Liquids*, 329 (2021) 115062.
3. Mohamed, N.M., Bashiri, R., Chong, F.K., Sufian, S. and Kakooei, S., *International Journal of Hydrogen Energy*, 40 (2015) 14031.
4. J.l.R. de Andrade, M.F. Oliveira, M.G. da Silva and M.G. Vieira, *Industrial & Engineering Chemistry Research*, 57 (2018) 3103.
5. S.-L. Chiam, S.-Y. Pung and F.-Y. Yeoh, *Environmental Science and Pollution Research*, 27 (2020) 5759.
6. Bashiri, R., Mohamed, N.M., Kait, C.F., Sufian, S., Kakooei, S., Khatani, M. and Gholami, Z. , *International Journal of Hydrogen Energy*, 99 (2016) 960.
7. H. Karimi-Maleh, M. Alizadeh, Y. Orooji, F. Karimi, M. Baghayeri, J. Rouhi, S. Tajik, H. Beitollahi, S. Agarwal and V.K. Gupta, *Industrial & Engineering Chemistry Research*, 60 (2021) 816.
8. G. Zhong, D. Liu and J. Zhang, *Journal of Materials Chemistry A*, 6 (2018) 1887.
9. S. Kang, L. Zhang, T. Xu, M. He, M. Chen, Q. Wang, D. Sun and X. Chang, *International Journal of Electrochemical Science*, 13 (2018)
10. M. Gurioli, Z. Wang, A. Rastelli, T. Kuroda and S. Sanguinetti, *Nature materials*, 18 (2019) 799.

11. J. Rouhi, M. Alimanesh, S. Mahmud, R. Dalvand, C.R. Ooi and M. Rusop, *Materials letters*, 125 (2014) 147.
12. S. Yuan, M. Wang and B. Lv, *International Journal of Electrochemical Science*, 15 (2020) 10731.
13. H. Karimi-Maleh, S. Ranjbari, B. Tanhaei, A. Ayati, Y. Orooji, M. Alizadeh, F. Karimi, S. Salmanpour, J. Rouhi and M. Sillanpää, *Environmental Research*, 195 (2021) 110809.
14. H. Zhang, N. Wang, S. Wang and Y. Zhang, *Physica E: Low-dimensional Systems and Nanostructures*, 117 (2020) 113806.
15. Z.N. Kayani, M. Sahar, S. Riaz, S. Naseem and Z. Saddiqe, *Optical Materials*, 108 (2020) 110457.
16. J. Rouhi, H.K. Malayeri, S. Kakooei, R. Karimzadeh, S. Alrokayan, H. Khan and M.R. Mahmood, *International Journal of Electrochemical Science*, 13 (2018) 9742.
17. D. Sharma and R. Jha, *Journal of Alloys and Compounds*, 698 (2017) 532.
18. D. Neena, M. Humayun, D. Lu, V.B. Mohan, D. Fu and W. Gao, *Ceramics International*, 46 (2020) 5278.
19. J. Rouhi, S. Kakooei, S.M. Sadeghzadeh, O. Rouhi and R. Karimzadeh, *Journal of Solid State Electrochemistry*, 24 (2020) 1599.
20. S.S. Ghoreishizadeh, X. Zhang, S. Sharma and P. Georgiou, *IEEE sensors letters*, 2 (2017) 1.
21. P. Salarizadeh, M.B. Askari, M. Seifi, S.M. Rozati and S.S. Eisazadeh, *Materials Science in Semiconductor Processing*, 114 (2020) 105078.
22. H.Q. Huynh, K.N. Pham, B.T. Phan, C.K. Tran, H. Lee and V.Q. Dang, *Journal of Photochemistry and Photobiology A: Chemistry*, 15 (2020) 112639.
23. G. Wu, G. Zhao, J. Sun, X. Cao, Y. He, J. Feng and D. Li, *Journal of catalysis*, 377 (2019) 271.
24. M.-S. Wu and J.-C. Lin, *Applied Surface Science*, 471 (2019) 455.
25. A. Sáenz-Trevizo, P. Amézaga-Madrid, P. Pizá-Ruiz, W. Antúnez-Flores and M. Miki-Yoshida, *Materials Research*, 19 (2016) 33.
26. G.D. Gesesse, C. Li, E. Paineau, Y. Habibi, H. Remita, C. Colbeau-Justin and M.N. Ghazzal, *Chemistry of Materials*, 31 (2019) 4851.
27. J. Rouhi, M.R. Mahmood, S. Mahmud and R. Dalvand, *Journal of Solid State Electrochemistry*, 18 (2014) 1695.
28. Z. Jiang, L. Feng, J. Zhu, X. Li, Y. Chen and S. Khan, *Ceramics International*, 46 (2020)
29. X. Li, B. Yang, C. Xu, J. Liu, W. Lu, S. Khan and L. Feng, *Journal of Materials Science: Materials in Electronics*, 30 (2019)
30. A. Phuruangrat, S. Siri, P. Wadbua, S. Thongtem and T. Thongtem, *Journal of Physics and Chemistry of Solids*, 126 (2019) 170.
31. S. Sa-nguanprang, A. Phuruangrat, T. Thongtem and S. Thongtem, *Russian Journal of Inorganic Chemistry*, 64 (2019) 1841.
32. V. Vaiano and G. Iervolino, *Catalysts*, 9 (2019) 964.
33. K. Umar, A. Aris, T. Parveen, J. Jaafar, Z.A. Majid, A.V.B. Reddy and J. Talib, *Applied Catalysis A: General*, 505 (2015) 507.
34. M. Shokri, G. Isapour, M.G. Hosseini and Q. Zarbpoor, *Water Environment Research*, 88 (2016) 2001.
35. M. Gholami, M. Shirzad-Siboni and J.-K. Yang, *Korean Journal of Chemical Engineering*, 33 (2016) 812.